Electronic Supplementary information

Dissociation and Hierarchical Assembly of Chiral Esters on Metallic Surfaces

Ben Moreton,[a] **Zhijia Fang,**[a] **Martin Wills**[a] **and Giovanni Costantini***[a]

Department of Chemistry, University of Warwick, Gibbet Hill Road,
Coventry, CV4 7AL, UK. E-mail: g.costantini@Warwick.ac.uk;
Tel: +44 24 765 24934

1. Synthesis of 1-(2'-Naphthyl)ethanol.

Note; the alcohol, which is a known compound [ESI.1-2], can be prepared in either enantiomeric configuration. Use of the (*R,R*)- enantiomer of catalyst gives the alcohol of *R*-configuration, whilst use of the (*S,S*)- enantiomer of catalyst gives the alcohol of *S*-configuration. Scheme ESI.1. illustrates the formation of the *S*- alcohol, which is the precursor of the ester (*S*)-NEP described in the main paper.
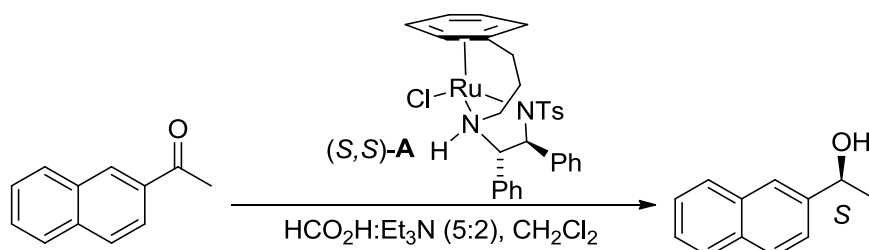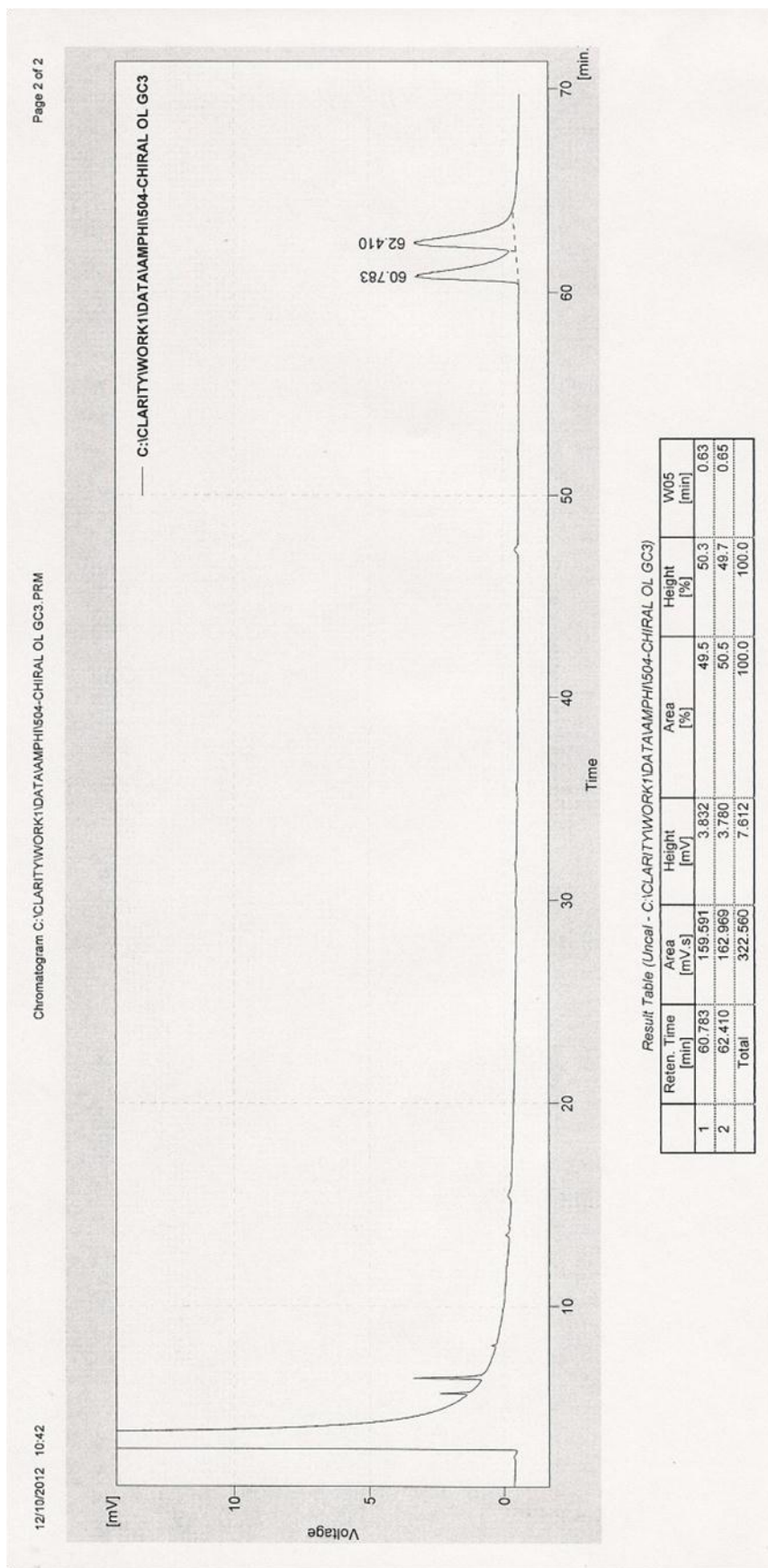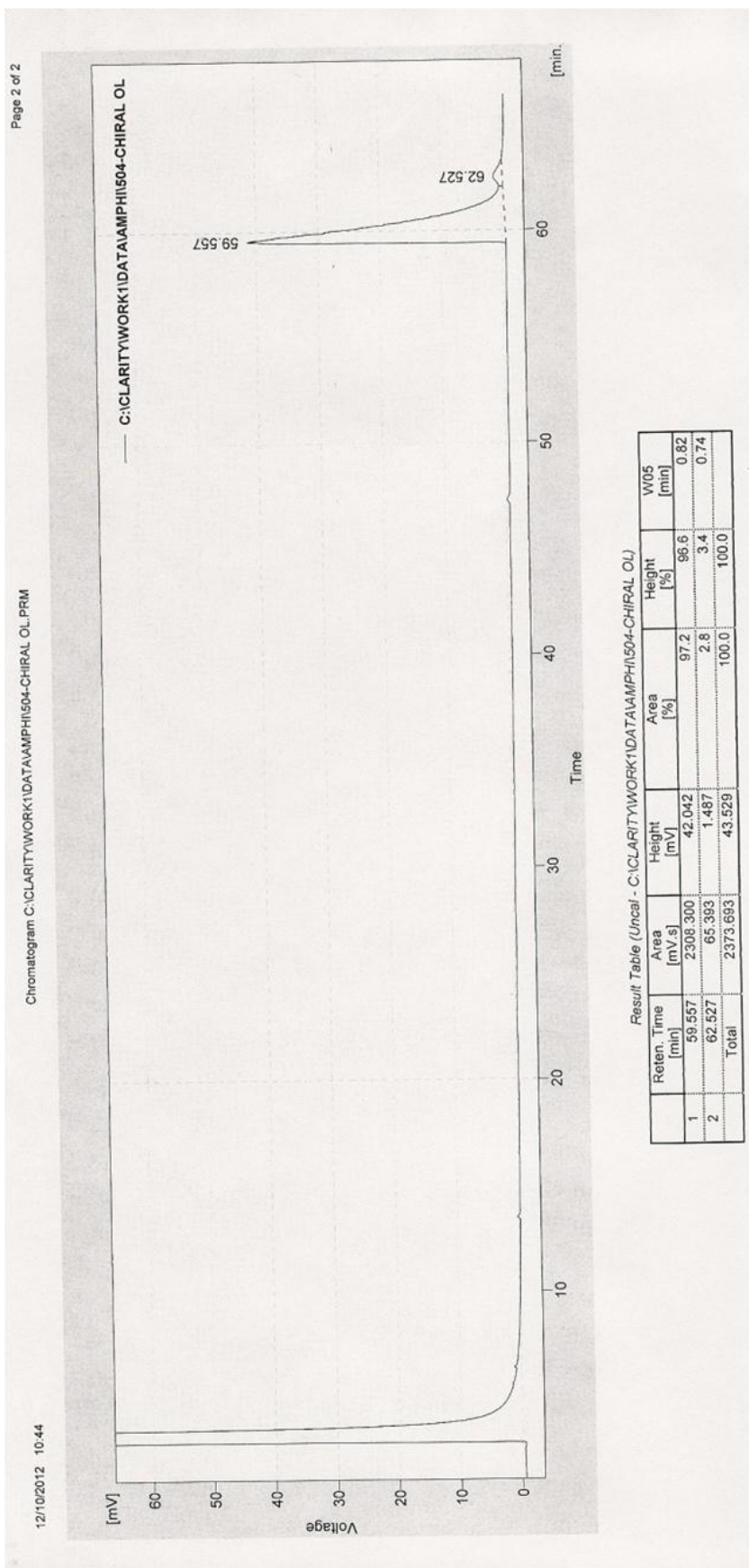

Scheme ESI.1.

(*R,R*)-Teth-TsDPEN-RuCl or (*S,S*)-Teth-TsDPEN-RuCl **A** [ESI.3] (0.6 mg, 1.0×10^{-3} mmol) was dissolved in HCO_2H/Et_3N 5:2 azeotropic mixture (840 mg, 0.59 cm^3) and 2-acetonaphthone (340 mg, 2.0 mmol) in degassed CH_2Cl_2 (2.0 cm^3) was injected under a nitrogen atmosphere. The mixture was stirred at 35 °C for 48 h then saturated aqueous $NaHCO_3$ (10 cm^3) was added. The reaction mixture was extracted with CH_2Cl_2 (3 × 20 cm^3), dried over anhydrous $MgSO_4$, concentrated and purified by silica gel column chromatography (eluent hexane/EtOAc=5:1) to give 1-(2'-naphthyl)ethanol as a white solid (334.4 mg, 1.94 mmol, 97%, 93% ee for *R*), (331.4 mg, 1.93 mmol, 96%, 93% ee for *S*). $[\alpha]_D^{24}$ + 37.8 (c 0.5 in EtOH), 93% ee (*R*). (Lit[1] $[\alpha]_D^{25}$ + 41.2 (c 0.50 in EtOH), 95% ee (*R*); Lit[2] $[\alpha]_D^{25}$ + 36.3 (c 0.58 in EtOH), 85% ee (*R*), δ_H (400 MHz, CDCl$_3$) 7.84-7.80 (4H, m, Ar), 7.51-7.44 (3H, m,

Ar), 5.06 (1H, qd, J 6.5, 3.6, CH), 1.93 (1H, brs, OH), 1.57 (3H, d, J 6.5 CH$_3$). HPLC separation conditions: CHIRALPAK IB column (30 cm x 6 mm) hexane:i-PrOH 96:4, 0.7 cm^3/min, T = 30 °C. Retention times, (S) 18.1 min, (R) 19.2 min. GC condition: Chrompac cyclodextrin-β-236M-19 50m, Carrier = hydrogen, T = 155 °C, P = 15 psi, Retention time for R isomer 60.8 min., Retention time for S isomer 62.4 min.
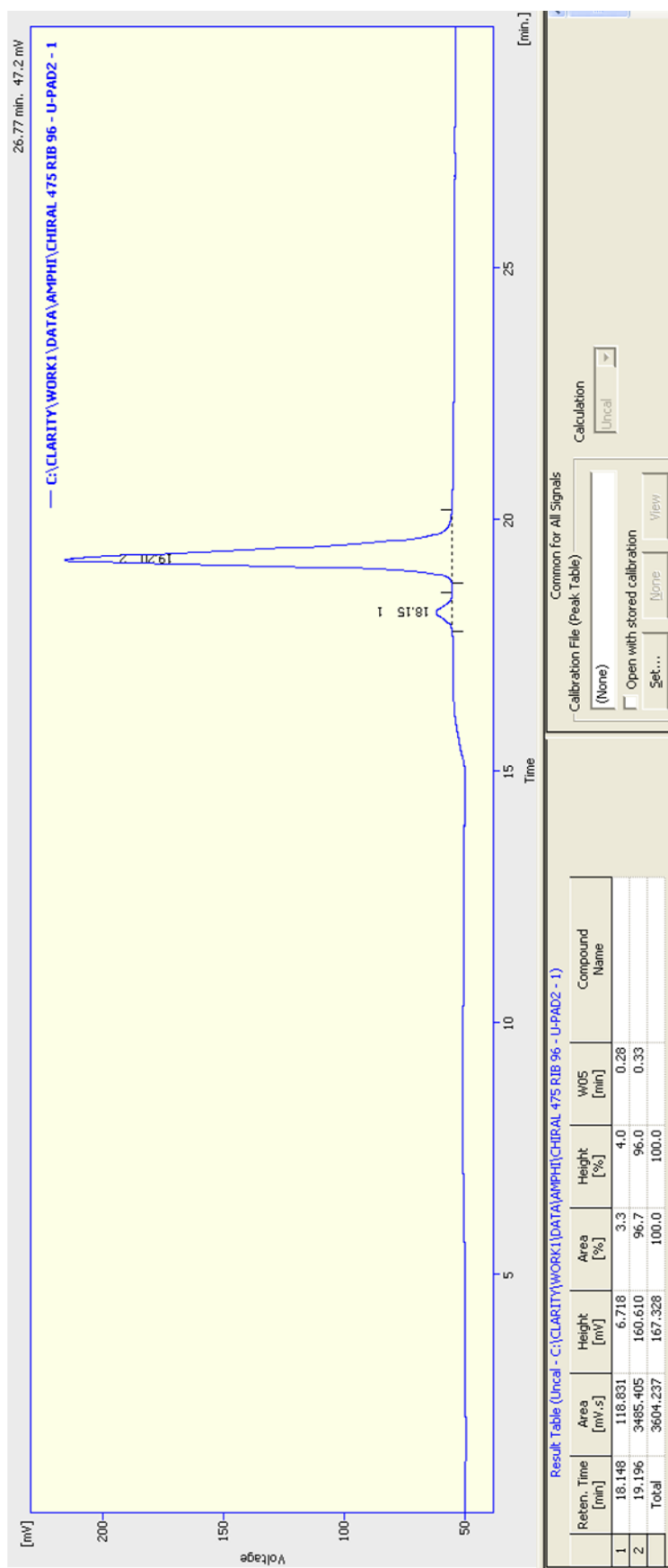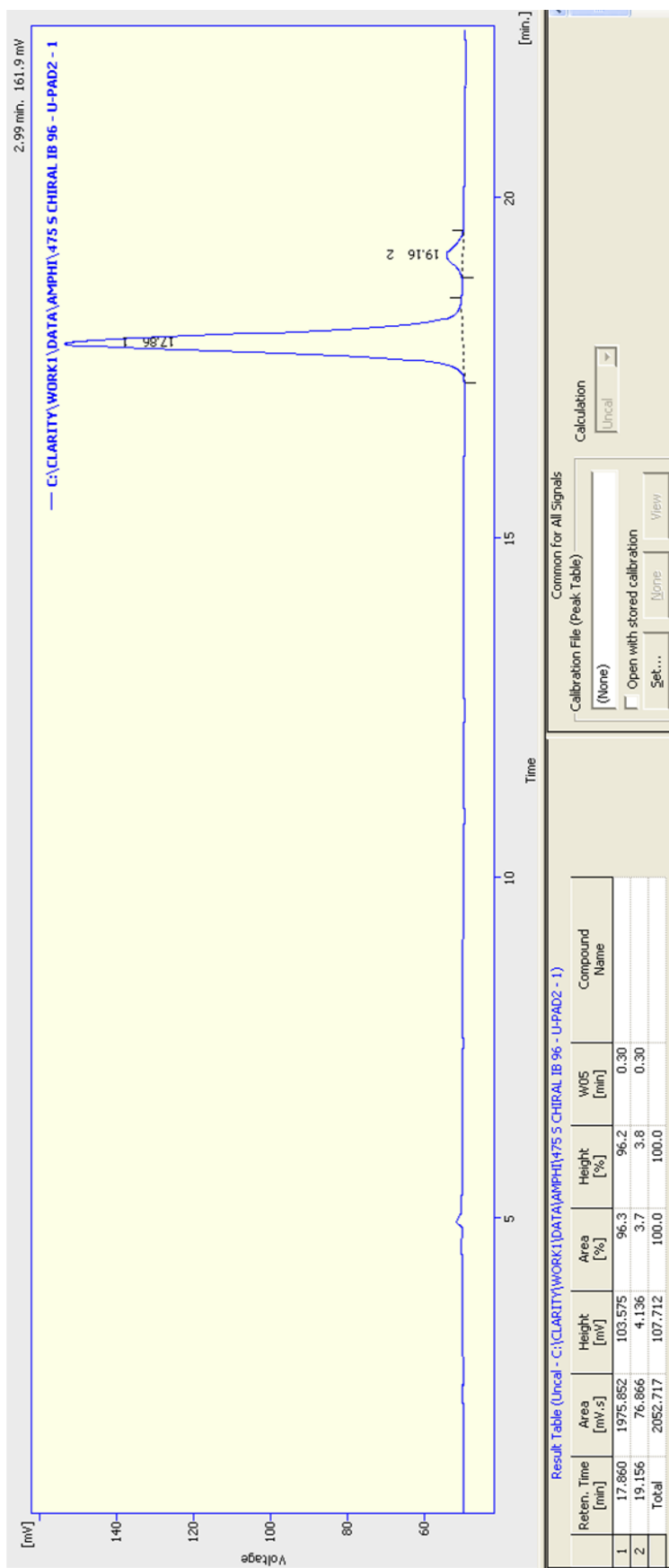
GC-Racemic alcohol.

C:\CLARITY\WORK1\DATA\AMPHI\I504-CHIRAL OL GC3

Chromatogram C:\CLARITY\WORK1\DATA\AMPHI\I504-CHIRAL OL GC3.PRM

12/10/2012 10:42

Result Table (Uncal - C:\CLARITY\WORK1\DATA\AMPHI\I504-CHIRAL OL GC3)

	Reten. Time [min]	Area [mV.s]	Height [mV]	Area [%]	Height [%]	W05 [min]
1	60.783	159.591	3.832	49.5	50.3	0.63
2	62.410	162.969	3.780	50.5	49.7	0.65
	Total	322.560	7.612	100.0	100.0	

3

GC-*R* enantiomer

Chromatogram C:\CLARITY\WORK1\DATA\AMPHI\504-CHIRAL OL.PRM

C:\CLARITY\WORK1\DATA\AMPHI\504-CHIRAL OL

12/10/2012 10:44

Result Table (Uncal - C:\CLARITY\WORK1\DATA\AMPHI\504-CHIRAL OL)

	Reten. Time [min]	Area [mV.s]	Height [mV]	Area [%]	Height [%]	W05 [min]
1	59.557	2308.300	42.042	97.2	96.6	0.82
2	62.527	65.393	1.487	2.8	3.4	0.74
Total		2373.693	43.529	100.0	100.0	

4

HPLC separation for *R-* enantiomer

Result Table (Uncal - C:\CLARITY\WORK1\DATA\AMPHI\CHIRAL 475 RIB 96 - U-PAD2 - 1)

	Reten. Time [min]	Area [mV.s]	Height [mV]	Area [%]	Height [%]	W05 [min]	Compound Name
1	18.148	118.831	6.718	3.3	4.0	0.28	
2	19.196	3485.405	160.610	96.7	96.0	0.33	
	Total	3604.237	167.328	100.0	100.0		

5

HPLC separation for *S*- enantiomer

Reten. Time [min]	Area [mV.s]	Height [mV]	Area [%]	Height [%]	W05 [min]	Compound Name
1	17.860	1975.852	103.575	96.3	96.2	0.30	
2	19.156	76.866	4.136	3.7	3.8	0.30	
Total		2052.717	107.712	100.0	100.0		

^{1}H NMR for alcohol.
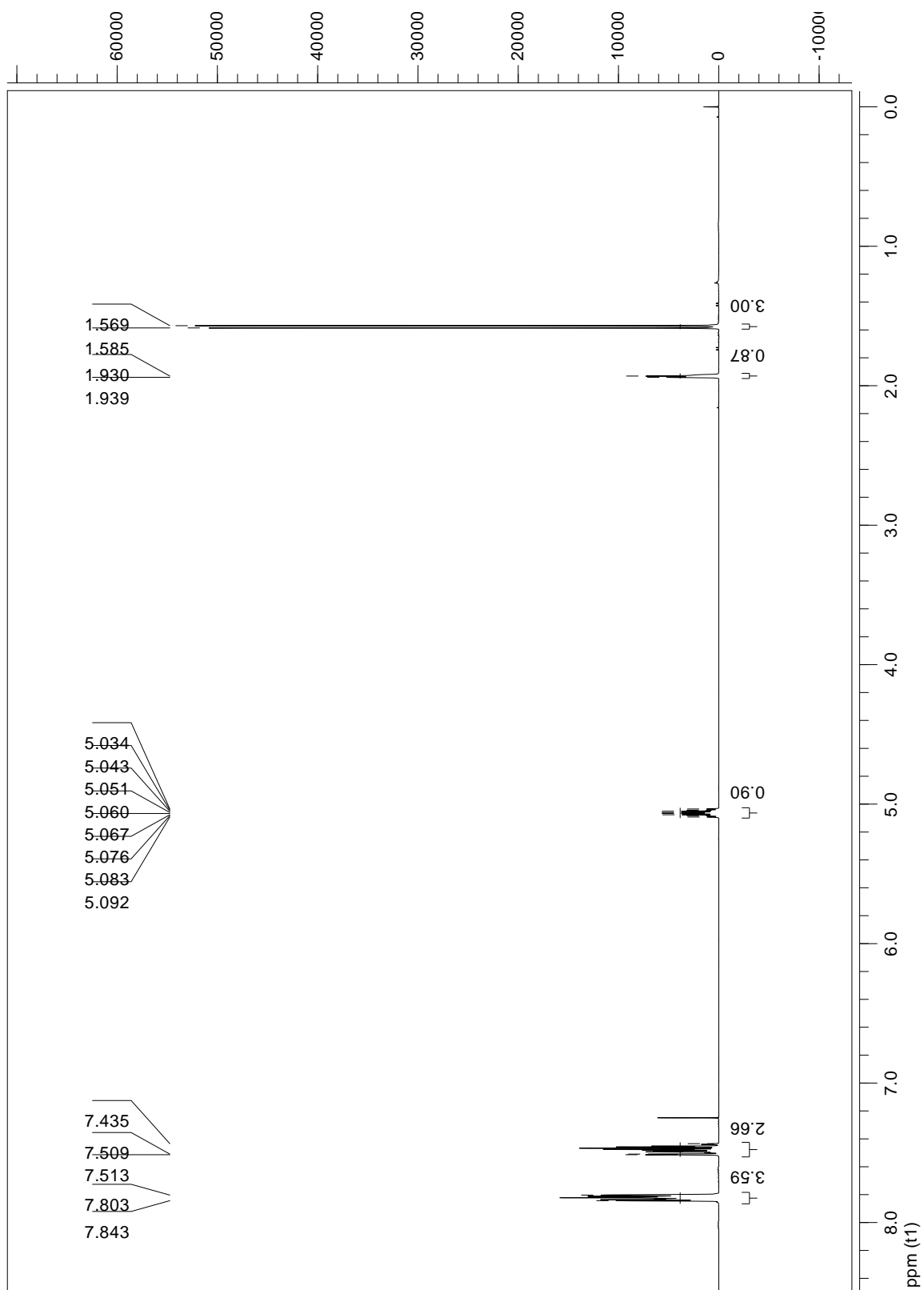
2. Synthesis of 1-(2'-Naphthyl)ethyl-(4-phenylbenzoate) (NEP).

Either enantiomer of the ester can be prepared, depending on the alcohol which is used. The configuration and enantiomeric purity of the product is unchanged upon esterification. The ester derived from the *S*- configuration alcohol was used in the work described in the main paper.
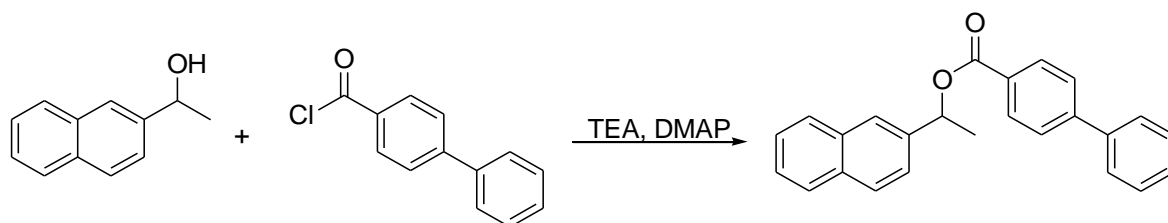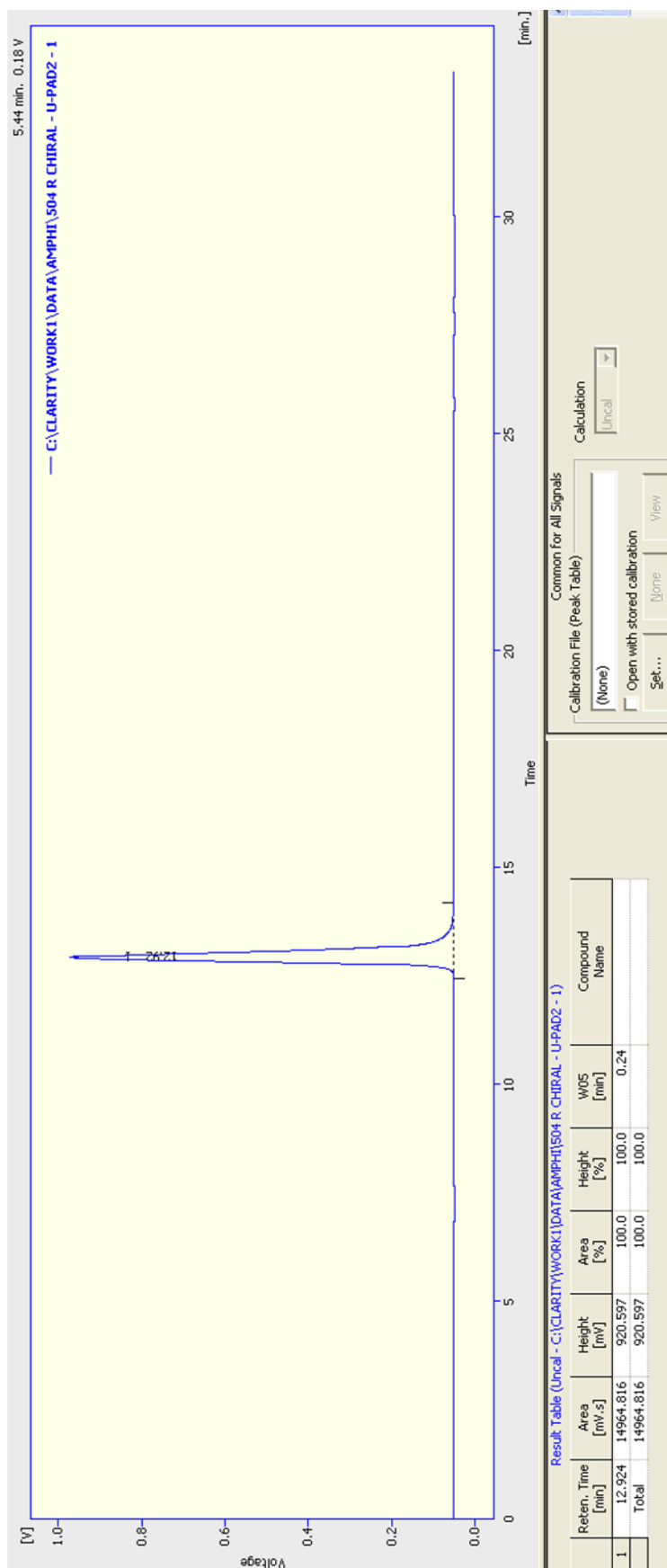

Scheme ESI.2

A solution of DMAP (catalytic amount, ca. 5 mg) and triethylamine (518 mg , 5.13 mmol) in CH_2Cl_2 (15 cm^3) was added dropwise to a solution of chiral 1-(2'-naphthyl)ethan-1-ol (294 mg, 1.71 mmol) and 4-phenylbenzoyl chloride (555 mg, 2.56 mmol) in CH_2Cl_2 (40 cm^3), at 0 °C. The reaction mixture was allowed to warm up to room temperature (RT) overnight and saturated aqueous $NaHCO_3$ (30 cm^3) was added. After stirring for 2 h, the organic phase was separated and further extracted with CH_2Cl_2 (2 × 40 cm^3). The combined organic phase was washed with brine (10 cm^3), dried over anhydrous $MgSO_4$, concentrated and purified by silica gel column chromatography (eluent hexane/ CH_2Cl_2/EtOAc=10:1:0.4) to give 1-(2'-naphthyl)ethyl-(4-phenylbenzoate) as a white solid (501 mg, 1.42 mmol, 82 % for *R*, 480 mg, 1.36 mmol, 80 % for *S*). $[\alpha]_D^{32}$ - 170.5 (c 0.5 in CHCl$_3$) >99% ee (*R*). $[\alpha]_D^{32}$ + 169.0 (c 0.6 in CHCl$_3$) >99% ee (*S*). Recrystallized samples were used for optical rotation measurements. MP 110 °C; (found (ESI): M$^+$ + Na, 375.1356. $C_{25}H_{20}O_2$ requires M, 375.1355); ν_{max} 1704, 1283, 1275, 745 cm^{-1}; δ_H (400 MHz, CDCl$_3$) 8.18-8.15 (2H, m, Ar), 7.90-7.81 (4H, m, Ar), 7.67-7.58 (5H, m, Ar), 7.50-7.37 (5H, m, Ar), 6.32 (1H, d, *J* 6.6, CH), 1.77 (3H, q, *J* 6.6, CH$_3$), δ_C (100 MHz, CDCl$_3$) 165.8, 145.7, 140.1, 139.2, 133.3, 133.1, 130.2, 129.3, 129.0, 128.5, 128.2, 128.1, 127.7, 127.3, 127.1, 126.3, 125.1, 125.1, 124.1, 73.1, 22.4. HPLC separation conditions: CHIRALPAK IB column (30 cm x 6 mm) hexane:*i*-PrOH 98:2, 0.6 cm^3/min, T = 30 °C. Retention times, (*R*) 12.8 min and (*S*) 23.1 min. A sample of the racemic alcohol was prepared by NaBH$_4$ reduction of 2-acetonaphthone and converted to the ester for HPLC analysis.
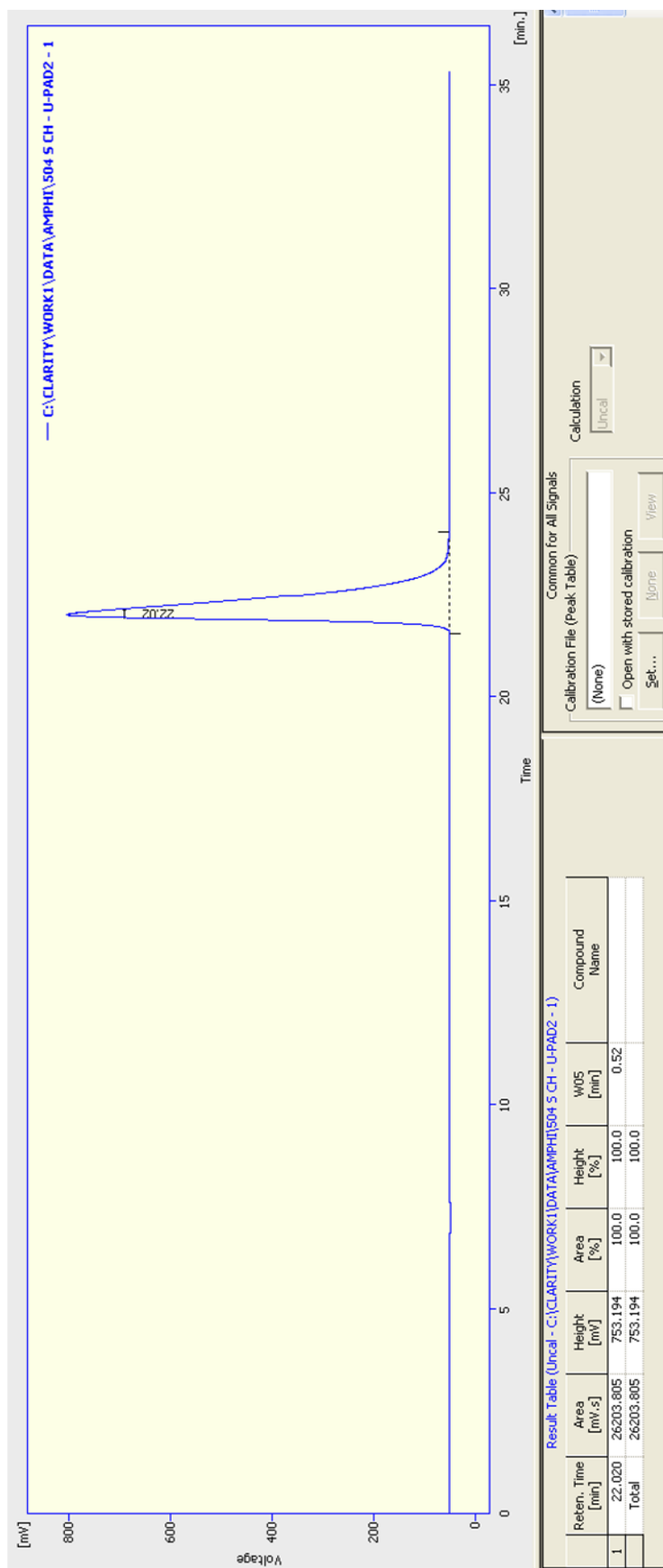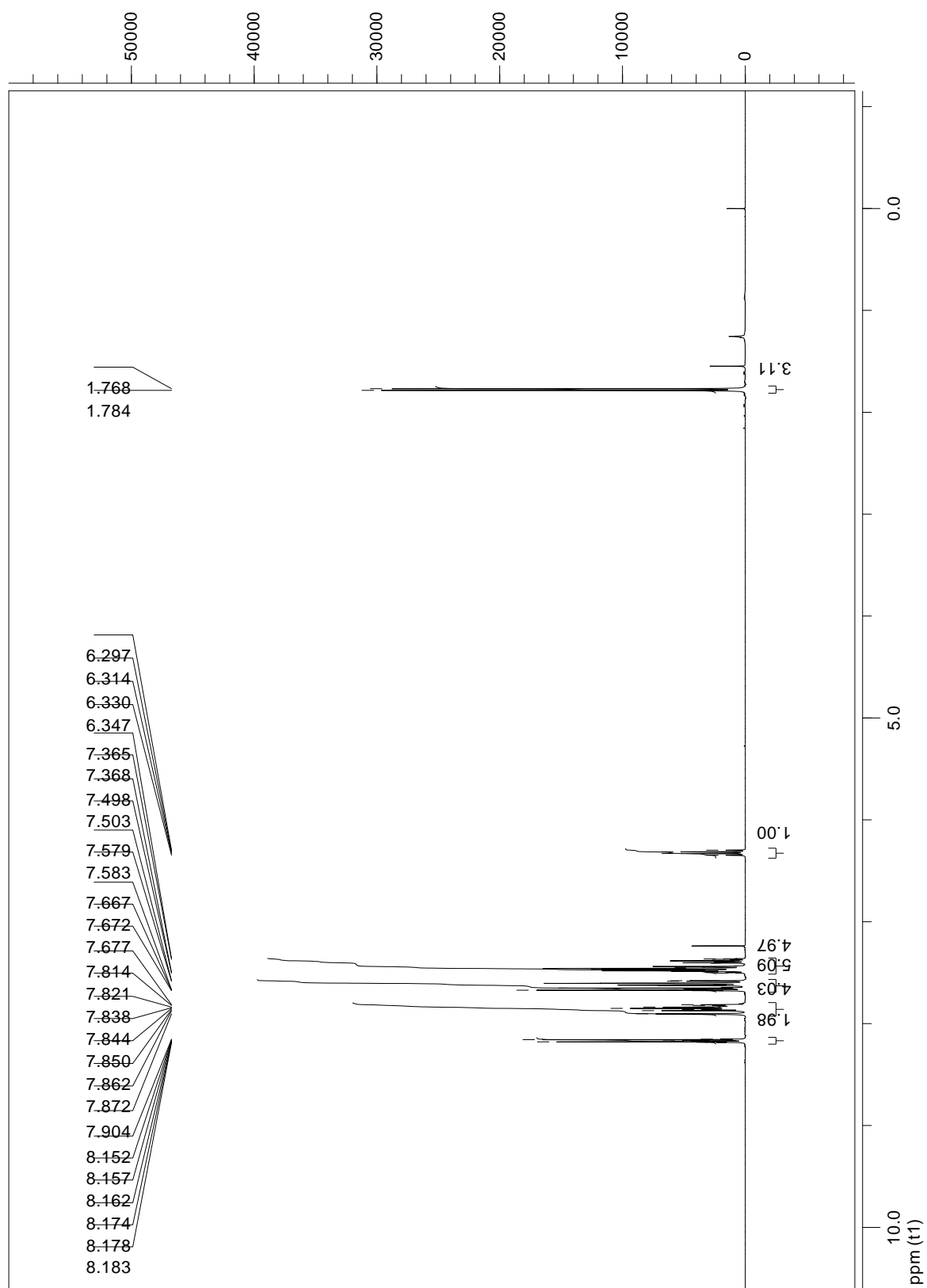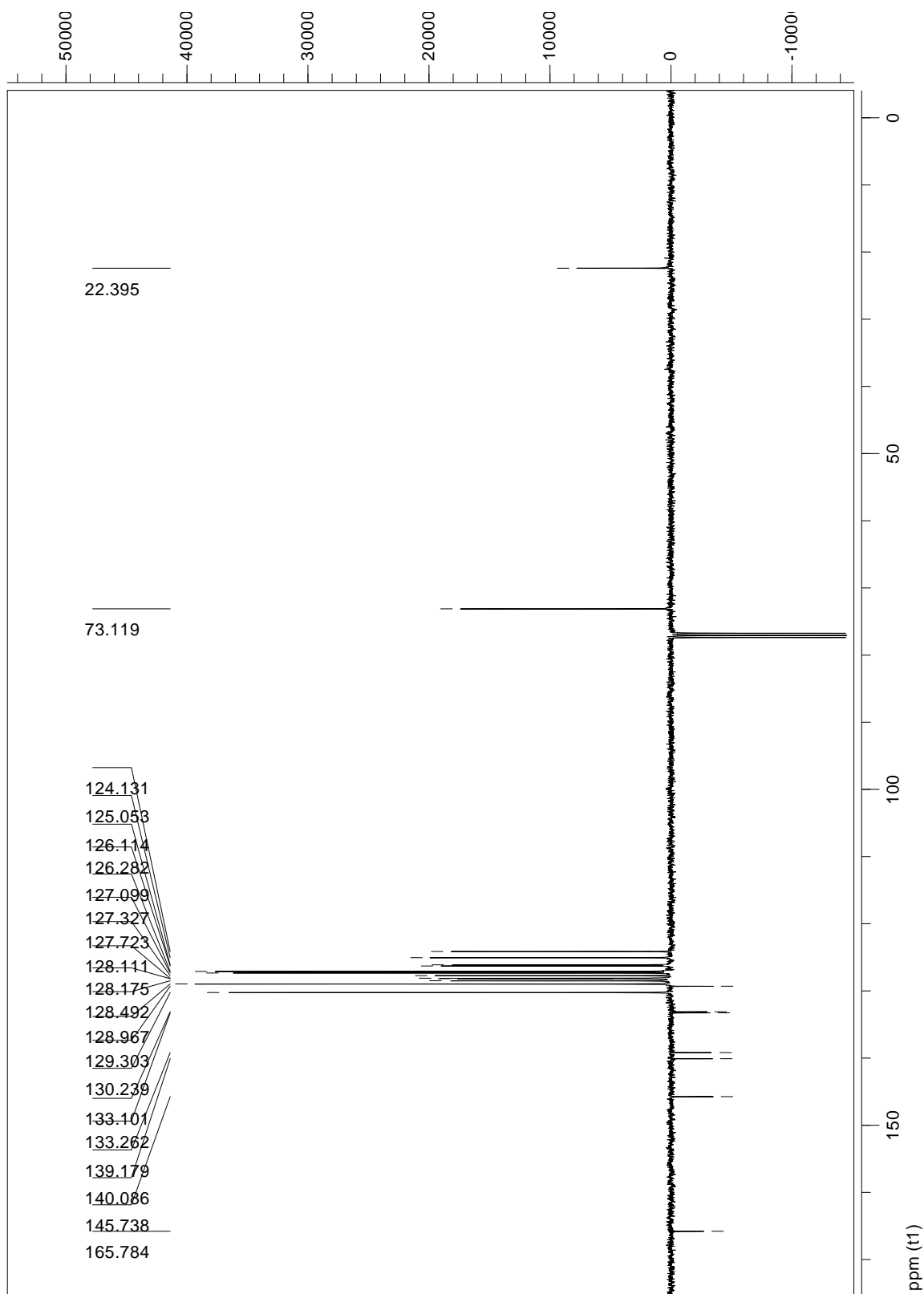
HPLC: Racemic ester.

Reten. Time [min]	Area [mV.s]	Height [mV]	Area [%]	Height [%]	W05 [min]	Compound Name
1	12.788	12564.954	873.677	48.7	71.0	0.22	
2	23.096	13236.407	357.255	51.3	29.0	0.56	
Total		25801.361	1230.932	100.0	100.0		

R-ester

Reten. Time [min]	Area [mV.s]	Height [mV]	Area [%]	Height [%]	W05 [min]	Compound Name
1 12.924	14964.816	920.597	100.0	100.0	0.24	
Total	14964.816	920.597	100.0	100.0		
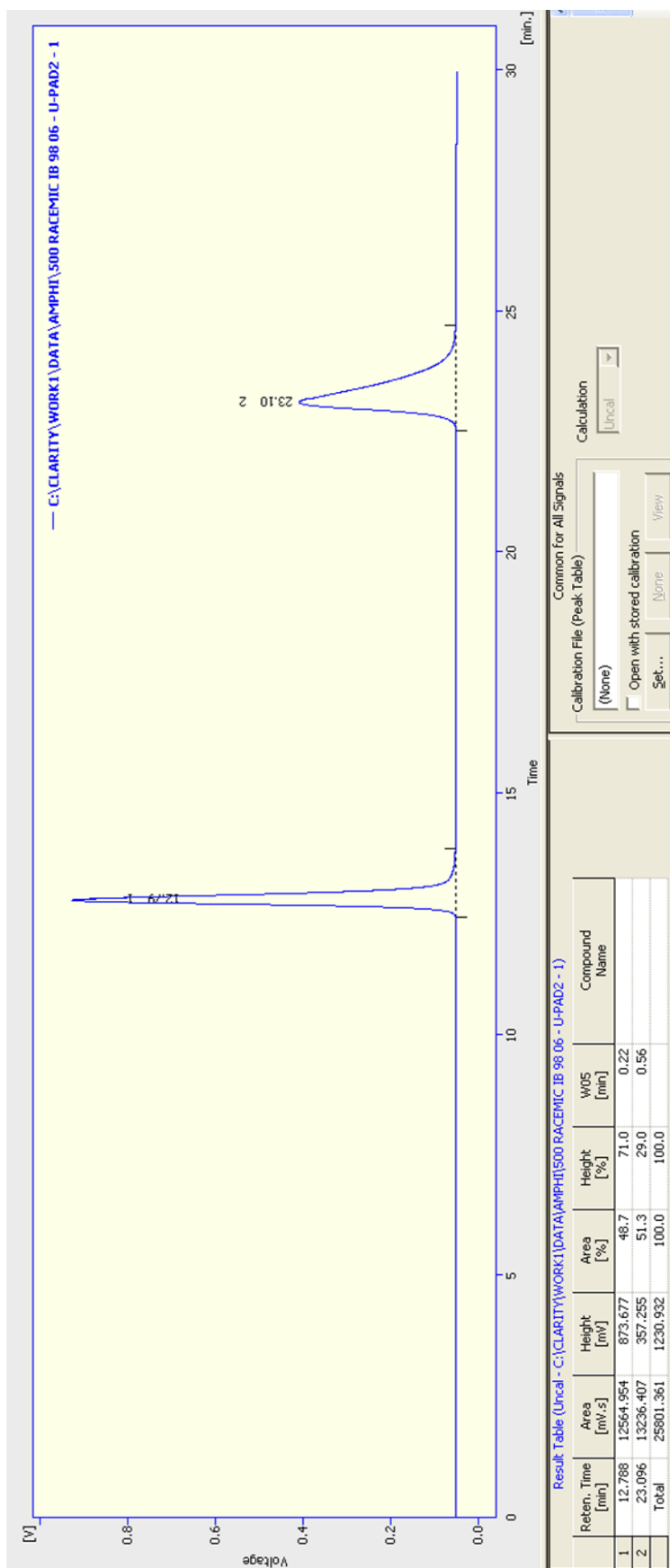
S-ester

¹H NMR of ester

^{13}C NMR of ester

50000 40000 30000 20000 10000 0 -1000

22.395

73.119

124.131
125.053
126.114
126.282
127.099
127.327
127.723
128.111
128.175
128.492
128.967
129.303
130.239
133.101
133.262
139.179
140.086
145.738
165.784

ppm (t1)

3. Sample Preparation and Imaging

The Cu(110) and Au(111) substrates were chosen as exemplary systems for reactive and unreactive substrates, respectively: Cu because of its use as catalysts for ester cleavage [ESI. 4, 5] and the (110) orientation as the most reactive among the low-Miller index planes; Au as an inert metal and (111) as the least reactive orientation. They were cleaned by cycles of Ar^+ sputtering (1 KeV, 6.5 µA, 5×10^{-5} mbar, 15 min) and annealing (Cu - 650°C, Au - 600°C, 2×10^{-9} mbar, 5 min). The NEP molecules were deposited onto the substrates by thermal sublimation from a Knudsen cell with a crucible temperature of 120°C for 10-30 min. Biphenylcarboxylic acid molecules were sublimed at 110°C for 2-5 min. The substrates were maintained at RT during deposition unless differently specified and then quenched to -196°C for imaging. Measurements were performed in a Createc UHV, low temperature STM system at -196°C with a base pressure of 4×10^{-11} mbar. Images were typically acquired at -1.3 V with a tunnelling current of 3×10^{-11} A. Errors in the STM evaluation of molecular sizes represent the standard deviation over a large statistics of data. All images were processed using the WsXM software [ESI.6].

4. NEP Fragmentation Paths

Before the experimental results are discussed, it is important to understand the possible products of the dissociation of NEP. Scheme ESI.3 shows the two possible cleavage locations, *a* and *b*, and the species resulting from fragmentation at those bonds. Cleavage at bond *a* will generate the two planer species, **2** and **3**, which are both stabilised by delocalisation effects. Molecule **2** is a prochiral species where the carbon rehybridises allowing delocalisation around the napthyl ring. The negatively charged carboxylate species **3** is symmetric and can be assumed to be stabilised in this form on the Cu(110) surface from comparison with similar benzene-carboxylic acids [ESI.7-11]. The cation **2** will most likely further deprotonate to the alkene **4**, producing an adsorbed free proton, whose fate depends on the specific substrate. On Cu(110), due to the aforementioned stabilisation of the carboxylate species, the free protons will most probably recombine and, after electron transfer from the metallic surface, desorb as molecular hydrogen. On the other hand, on the less reactive Au(111) it is expected that, because of the proximity of the two groups, the proton transfers to the carboxylate **3**, protonating it to the acid, **5** (see main text).

Cleavage at bond *b*, as suggested by reference [ESI.5], will create the two radicals, **6** and **7**, neither of which can be further stabilised via delocalisation effects. Radical **7** is chiral while radical **6** is prochiral.

In summary, the most likely cleavage of ester NEP is at position *a* because this will generate the most stable products based on their stabilisation from delocalisation.
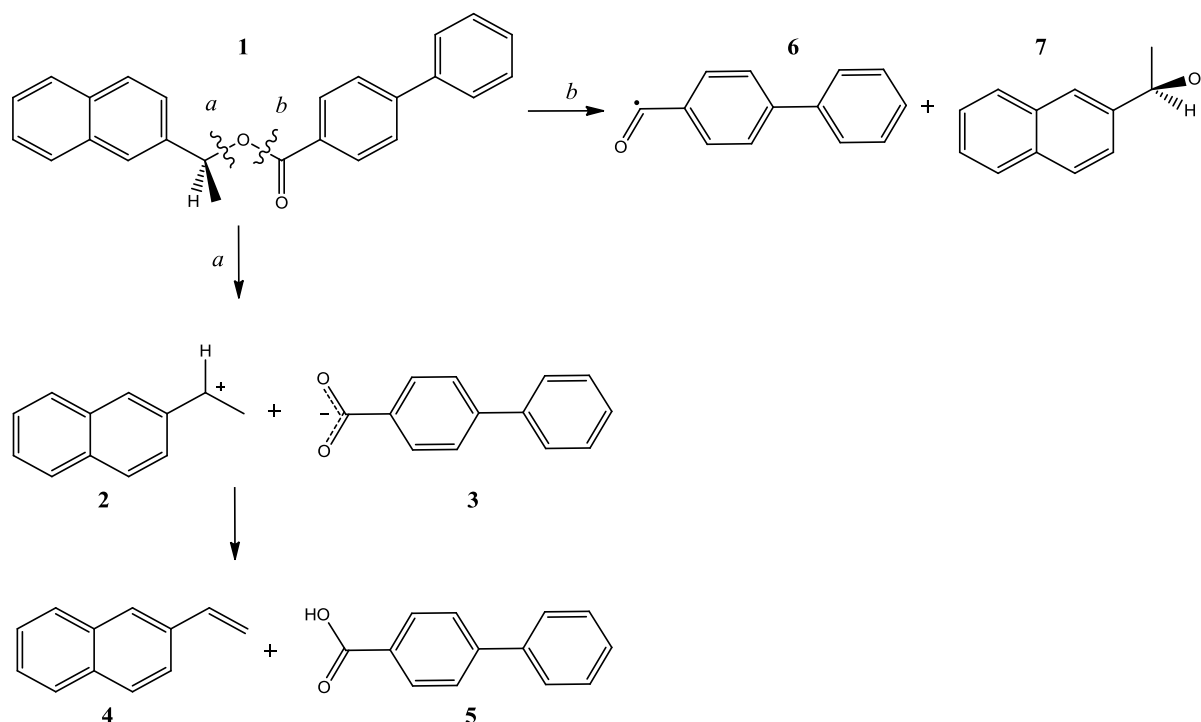
Scheme ESI.3 The two possible fragmentation pathways of NEP.

5. Sublimation tests

5.1. Sublimation Test of NEP

Since NEP is a relatively large molecule, there is the possibility it dissociates even before surface adsorption, due to thermal decomposition during sublimation. For this reason the electrospray ionisation mass spectra of the pristine molecule and the molecule recovered from a glass slide after vacuum sublimation were compared.

NEP was sublimed onto a glass microscope slide from a Knudsen cell with a crucible temperature of 120°C at a base pressure of 2×10^{-6} mbar. The electrospray ionisation mass spectra (ESI-MS) were recorded both for the molecules before sublimation, figure ESI.1(a), and for the material recovered from the glass slide, figure ESI.1(b). The two ESI-MS show the same two peaks corresponding to the molecular peak, 375, and the cationic 2-ethyl naphthalene fragment, **2**, 154.9, resultant from a cleavage at the $RCH(CH_3)$-$OC(O)R$ bond. The presence of the cationic fragment in the reference spectra, prior to sublimation, indicates that it is generated by the ionisation process. Since the peak ratios are reasonably equivalent between the two spectra in figure ESI.1, we deduce that the molecule has not decomposed during sublimation.
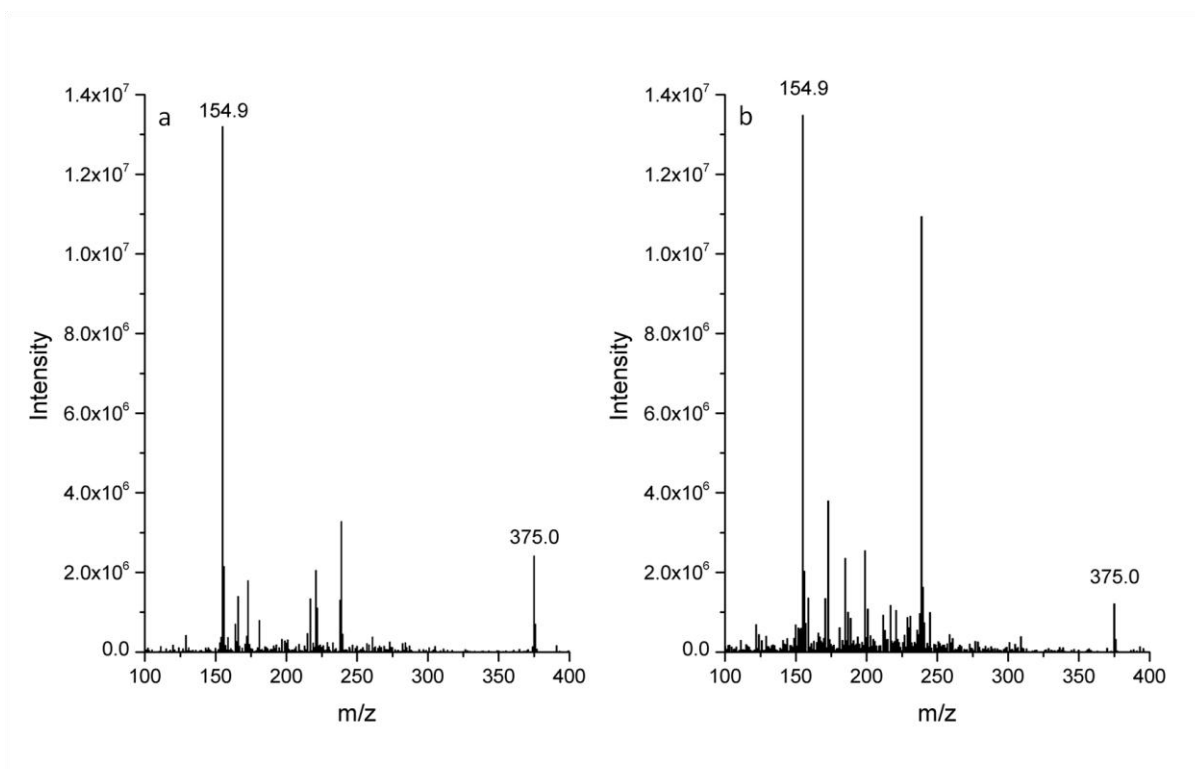
16

Figure ESI.1 Electrospray mass spectra of NEP (a) prior to and (b) after heating to 120°C. Apart from the solvent contamination peaks between 160 and 360 m/z that appear at different intensities (e.g. the peak at 238.9 m/z), the two spectra are identical showing the molecule has not decomposed during sublimation.

5.2. Sublimation test of possible fragment species

Cleavage along the RO-C(O)R bond

Based on the calculations by Santiago et al. [ESI.5], esters should dissociate along the RO-C(O)R bond on Cu substrates to generate the radicals **6** and **7** in scheme ESI.3. Since the radical **7** could not exist outside of our experimental environment, we decided that the molecule 1-(2-naphthyl)ethanol (**8** in scheme ESI.4) would be the best analogue. This is because, in particular upon deposition on the reactive Cu(110) substrate, **8** could be expected to deprotonate thereby generating a similar species to **7**. However, after maintaining the alcohol **8** at a vacuum of 2×10^{-6} mbar for one hour at room temperature, the molecule had visibly evaporated such that there were no longer molecules present in the crucible. This indicates that the vapour pressure of **8** is too high for this molecule to be deposited in UHV through a Knudsen cell. The molecule was therefore not analysed.

17

The analogue for the complementary fragment, radical **6**, is more difficult to create. Deposition of biphenyl-4-carbonyl chloride (**9** in scheme ESI.4) could, in theory, be a candidate, although the relatively high annealing temperature required to dissociate the chlorine is expected to induce molecular coupling via an Ullman reaction [ESI.12]. As a consequence, this molecule was also not analysed further.

Cleavage along the RCH(CH₃)-OC(O)R bond

If, on the other hand, the NEP molecule cleaved along the $RCH(CH_3)-OC(O)R$ bond, the resulting fragments would be **2** and **3**. As discussed in section 4, these may undergo H-transfer to the alkene 2-vinylnaphthalene **4** and the biphenylcarboxylic acid **5**, respectively.

Although alkene **4** was also planned to be deposited on Cu(110) and Au(111), its melting temperature is around 64-68°C, i.e. even lower than that of **9** (70-71°C). The alkene **4** is thus expected not to be stable under vacuum conditions either.

The complementary fragment of this cleavage, namely the biphenylcarboxylic acid **5** was stable under vacuum and analysis by ESI-MS showed that it sublimed intact. As the only suitable molecule of the four possible fragments, it was chosen for comparative imaging with NEP.
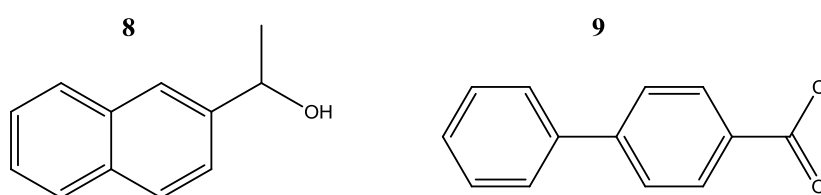
Scheme ESI.4. **8** 1-(2-naphthyl)ethanol and **9** biphenyl-4-carbonyl chloride.

6. Biphenylcarboxylate fragment

6.1. Deposition of biphenylcarboxylic acid onto Cu(110)

Upon deposition onto a Cu(110) substrate maintained at room temperature, the biphenyl-carboxylic acid **5** appears as symmetric oblong features which align along the [001] and

[1$\bar{1}$0] directions of the surface and assemble in different types of supramolecular structures (figure ESI.2(b)). The biphenyl molecules are believed to have deprotonated [ESI.7-11] and to be mutually bonded by ionic hydrogen bonds between the carboxylate and aromatic hydrogens, figure ESI.4(a). The inclusion of Cu adatoms in the observed supramolecular structures cannot be excluded, as reported for similar benzene-carboxylic acids on Cu(110) [ESI.8-10].

The structures formed by **5** upon adsorption on Cu(110) bear several similarities with those observed for the deposition of NEP under the same conditions (figure ESI.2(a)). The main types of aggregates are highlighted in figure ESI.3 for both the NEP (upper row) and acid (lower row) depositions. It can be easily recognised that all but one of the aggregation states observed in the NEP sample are also seen in the acid one.

It should however be noted that in figure ESI.2(b) only aggregates of molecules are observed whereas in figure ESI.2(a) there are also isolated monomers. These monomers are mainly attributed to the complementary alkene species **4** after fragmentation of NEP, see section 4 .
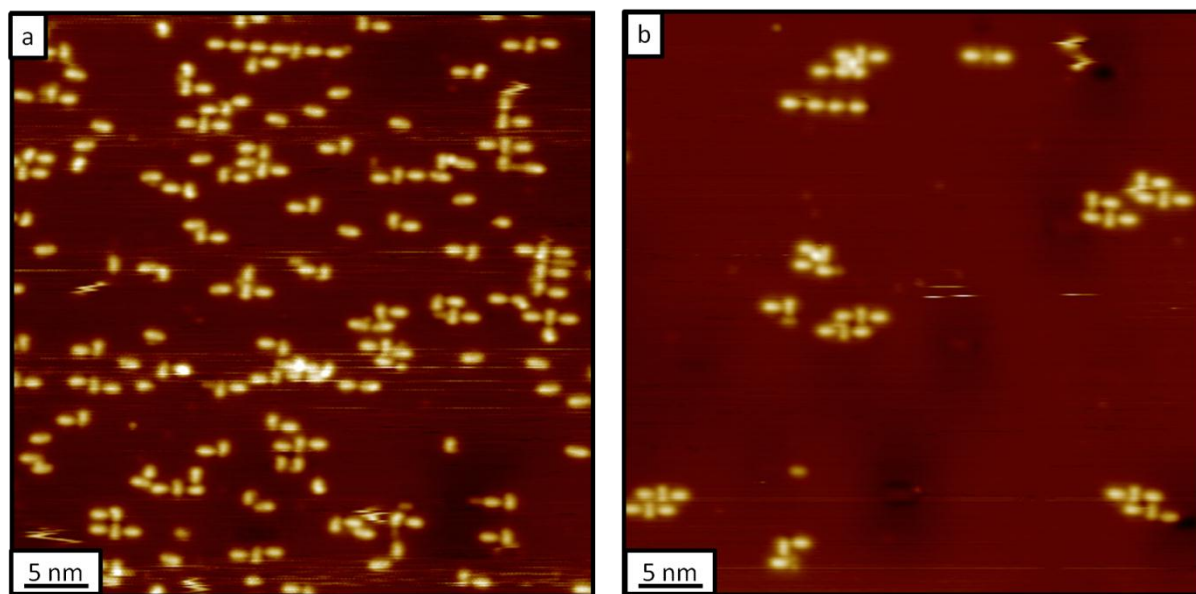

Figure ESI.2. STM images of (a) NEP and (b) biphenylcarboxylic acid deposited at room temperature on Cu(110) showing similar assembly patterns. The images were acquired at -196°C.
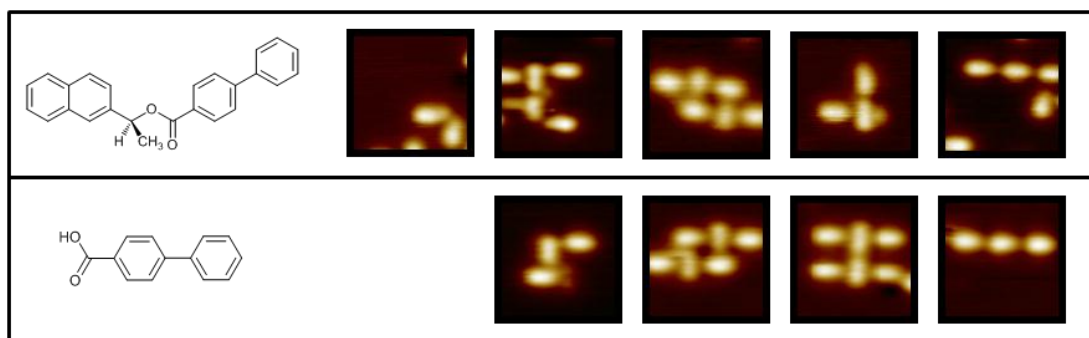
19

Figure ESI.3. Main types of assemblies observed after deposition of NEP (upper row) and biphenylcarboxylic acid (lower row) onto Cu(110). Clear analogies can be readily recognised between the observed structures.

6.2. Proposed Aggregation Model for the Structures Observed in the NEP Sample

A model for one of the aggregates observed in the NEP sample (figure ESI.2(a) and upper row of ESI.3) is proposed in figures ESI.4(b) and (c), based on the assumption that the individual molecular units are the biphenylcarboxylate **3** or the radical **6** deriving from the cleavage of the RCH(CH$_3$)-OC(O)R and the RO-C(O)R bonds, respectively. This specific aggregate was chosen as an example because it shows both the head-to-head and the perpendicular bonding motifs which are recurring in all of the aggregates. However, a similar comparison can be made for all the other binding motifs displayed in figure ESI.3. The directionality of the ionic H-bonds in the carboxylate fragment has a good match with the observed structure for both the vertical and parallel interactions. While it would in theory still be possible to generate analogous structures with the radical fragment **6**, the corresponding H-bonds would be much weaker. In particular, the head to tail assembly would be stabilised by a very weak interaction and would be expected to be more offset than what is actually observed. Moreover, while the two H-bonds of the carboxylate fragment would allow only the actually observed relative positions of the individual molecules as displayed in figure ESI 4(b), the single H-bond of a possible carbonyl radical would result in several other configurations.

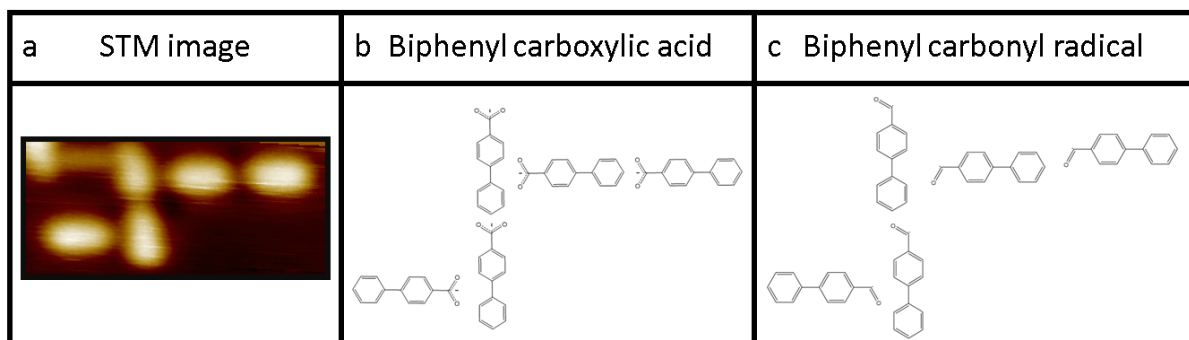| a	STM image	b	Biphenyl carboxylic acid	c	Biphenyl carbonyl radical

Figure ESI.4. (a) STM image of a representative NEP fragment aggregate. (b) and (c) Models showing the proposed H-bonding motifs for the (b) deprotonated biphenylcarboxylic acid **3** and (c) biphenyl carbonyl radical **6** resulting from the NEP cleavage along the RCH(CH₃)-OC(O)R and the RO-C(O)R bonds, respectively.

7. Origin of Mirror Symmetric Species Observed in the Dissociated NEP Sample

With a good tip condition, some of the isolated molecular species within the dissociated NEP/Cu(110) sample appear as mirror symmetric, see figure ESI.5. These species typically have the shorter of the two measured lengths, i.e. 11.5 ± 0.4 Å, and are observed to align mainly along the $[1\bar{1}0]$ direction but can also be found along $[001]$. The fact that they appear in two mirror symmetric configurations strongly indicates that they are the same prochiral molecule in two different adsorption orientations. Out of the possible fragments identified in scheme ESI.3, only two are prochiral, namely species, **4** and **6**, the first one resulting from the cleavage of the RCH(CH₃)-OC(O)R bond, the latter from the cleavage of the RO-C(O)R bond.

If the molecules in figure ESI.5 were to be assigned to species **6**, then the complementary fragment **7** should also be observed. But this is not the case since **7** is chiral and there is no evidence for any chiral species in the STM data. Moreover, even with the best tip conditions, symmetric oblong species (as those reported, e.g., in the upper row of figure ESI.3) are always observed to coexist with the prochiral species. Neither **6** nor **7** possess this symmetry, therefore strongly supporting the idea that the NEP cleavage cannot happen along the RO-C(O)R bond.

On the other hand, the experimental observations are nicely explained by a cleavage along the RCH(CH₃)-OC(O)R bond, since this would produce molecules **4** and **3** which are prochiral and symmetric, respectively.
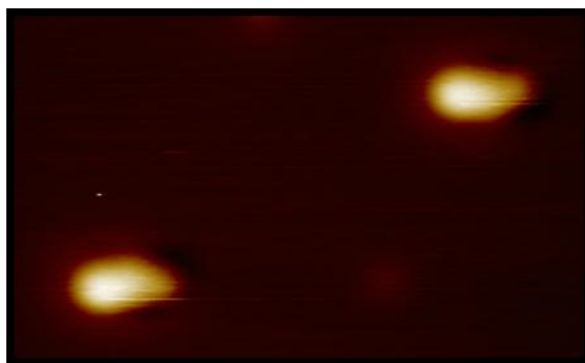
21

Figure ESI.5. STM image of two mirror symmetric species observed on the dissociated NEP after deposition at room temperature on Cu(110).

8. Origin of the Two Main Configurations Observed for the Low Temperature Deposition of NEP on Cu(110)

When deposited onto a Cu(110) substrate held at -130°C, the NEP molecules either fragment (20% of the population), or adsorb intact (80%) and appear as two lobes, one larger than the other, linked by a bright protrusion. Of the intact molecules, 45% have a conformation where the two lobes make an angle of 90° to one another, 35% have an angle of 130° and 10° have an angle of 180°. The two major conformations, namely the 90° and 130°, can be explained by a rotation of 180° about the naphthalene–CCH$_3$O bond shown in figure ESI.7. This changes the angle that the biphenyl and naphthalene groups make with one another.

Gas phase calculations of the energies for these two configurations were performed using the AM1 method in the GAMESS software [ESI.13]. The energies were minimised until a difference of 1.0×10^{-6} Hartree was obtained for successive iterations. The energies obtained were –4115.712992 eV and –4115.716639 eV for the 130° and 90° orientations, respectively. The difference of about 4 meV implies that these two configurations are essentially energetically identical in the gas phase.
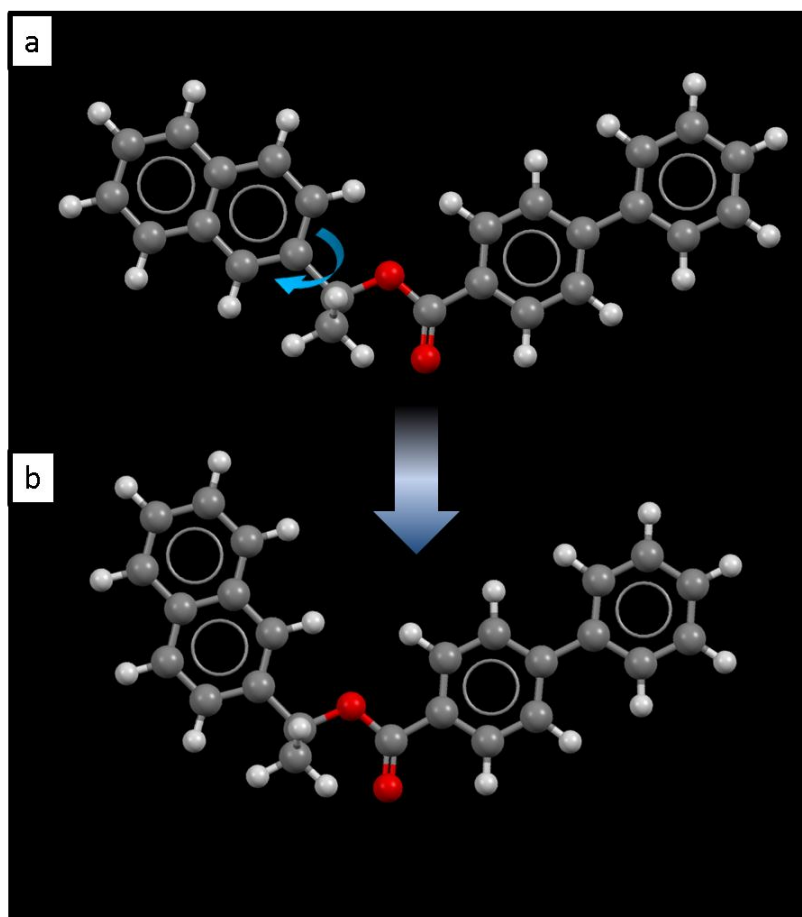
Figure ESI.7. A 180° rotation about the naphthalene – CCH$_3$O bond, highlighted by the curved arrow in (a), alters the conformation of the molecule: (a) 130° and (b) 90° between the biphenyl and the naphthalene groups.

9. Appearance of intact NEP

Differently to figures 1(c), 2(b) and 2(d), in figure 1(d) of the main text the intact NEP molecule is imaged without a bright spot at the position of the methyl group. We exclude that this is due to NEP adsorbing with the methyl group directed towards the surface, since this would result in a mirror symmetric appearance of the molecule which was never observed. Alternatively, it could be argued that the molecules have fragmented but are still held in an L-shaped configuration because of H-bonding. This is also thought to be unlikely because individual fragments are observed on the surface too (20%), indicating that the barrier for their separation is low. Moreover, manipulation of the molecules by the STM tip showed that they translate and rotate as a single entity and do not split into two separate features (figure ESI.8).

10. Manipulation of NEP Molecules with the STM Tip

In order to manipulate the NEP molecules, the STM tip was brought very close to the surface by increasing the tunnelling current to 8×10^{-9} A and reducing the bias to -0.09 V (typical imaging conditions are 3×10^{-11} A and -1.3 V). The scanning rate was maintained at 3 Hz. Images before and after manipulation are shown in figure ESI.8, where immobile molecules are used as a reference and are circled in red while the moving molecules are circled in blue. Both translation and rotation of whole molecules were observed, strongly indicating that the molecules have not fragmented.
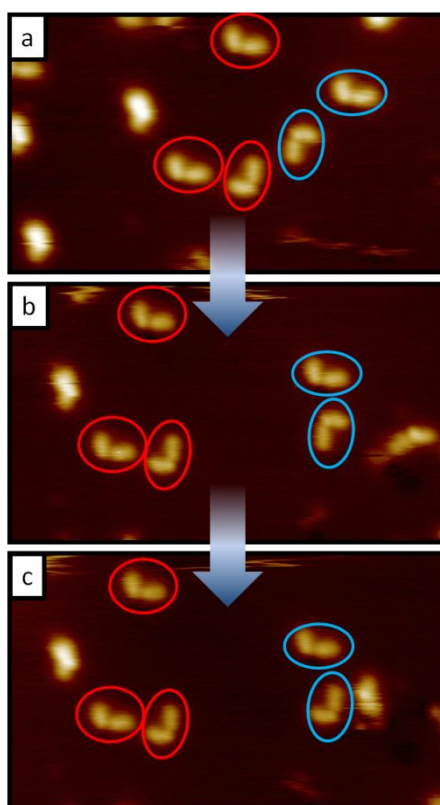

Figure ESI.8. Successive STM images after manipulation of the NEP molecules by the STM tip. The molecules circled in blue translate with respect to the molecules circled in red from (a) to (b). The lower of the blue molecules rotates from (b) to (c). Few unidentified fragments are also visible within the images. All images were acquired at -196°C.

11. Intermediate NEP Coverage on Au(111)

At less than monolayer coverage, the NEP molecules are highly mobile on Au(111) and most of them appear as blurry features in the STM images, figure ESI.9. The moving molecules have a wavelike pattern which indicates that they are bound by the herringbone reconstruction of the Au(111) surface. Some of the stable aggregates appear as small domains of the six-pronged star structures described in the main text while others have fragments at their core.

Only when the coverage is further increased to about a full monolayer, extended stable structures are formed, with the NEP molecules arranged into chiral hierarchic supramolecular architectures, as shown in figure 2(a) in the main text. However, unlike on Cu, only the configuration with an angle of about 90° between the two lobes is observed, implying that the interaction with the Au substrate favours one of the two possible rotations around the naphthalene – CCH_3O bond (figure ESI.7).
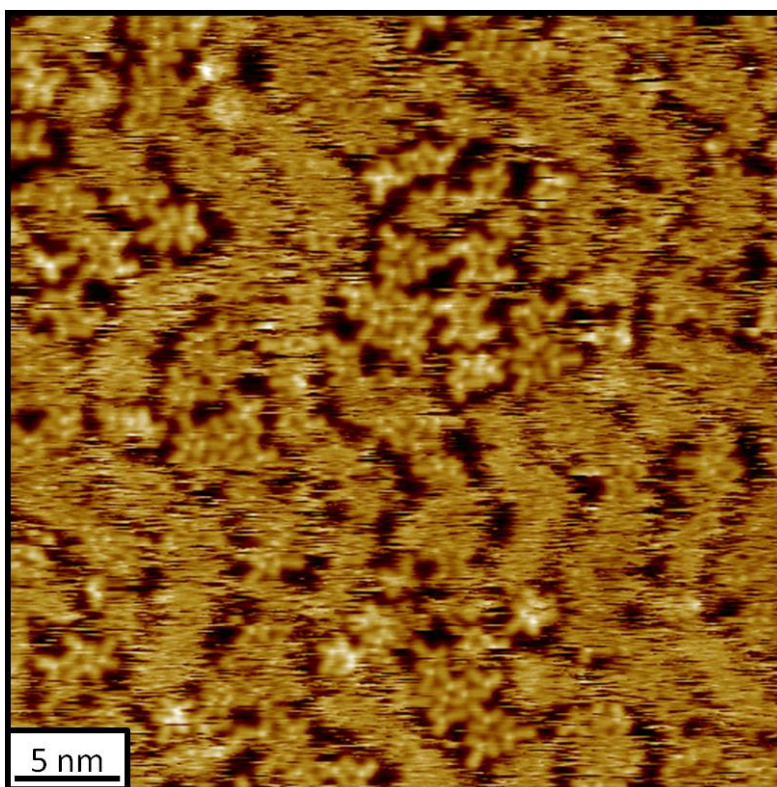

5 nm

Figure ESI.9. STM image of intermediate coverage of NEP on Au(111). The molecules are confined by the herringbone reconstruction however most of them are too mobile to be effectively imaged at −196°C.

12. Deposition of Biphenylcarboxylic Acid on Au(111)

Deposition of the biphenylcarboxylic acid onto Au(111) at room temperature yields several structures. The majority of these are three-, four- and five-pronged stars which show organisational chirality (figure ESI.10(c)) presumably based on H-bonding between still protonated molecules. The acid molecules also form 2D chains (figure ESI.10(d)) where two molecules H-bond in a head to head fashion to generate a supramolecular monomer which then form chains, presumably via secondary H-bonding. Comparison with the NEP measurements shows that the three-pronged stars at the core of the triangular assemblies observed after 100°C annealing of NEP (figure ESI.10(a)) are identical to the three-pronged stars formed by biphenylcarboxylic acid (figure ESI.10(b)). This clearly demonstrates that the NEP fragments observed at high temperatures on Au(111) are still protonated biphenyl-carboxylic acid. As mentioned above, the three pronged stars in the biphenylcarboxylic acid sample show organisational chirality, figure ESI.6(c). However the stars at the centre of the triangles in the NEP sample show only one chirality (figure ESI.10(a)), indicating that the NEP molecules have a templating effect on the acid structures.
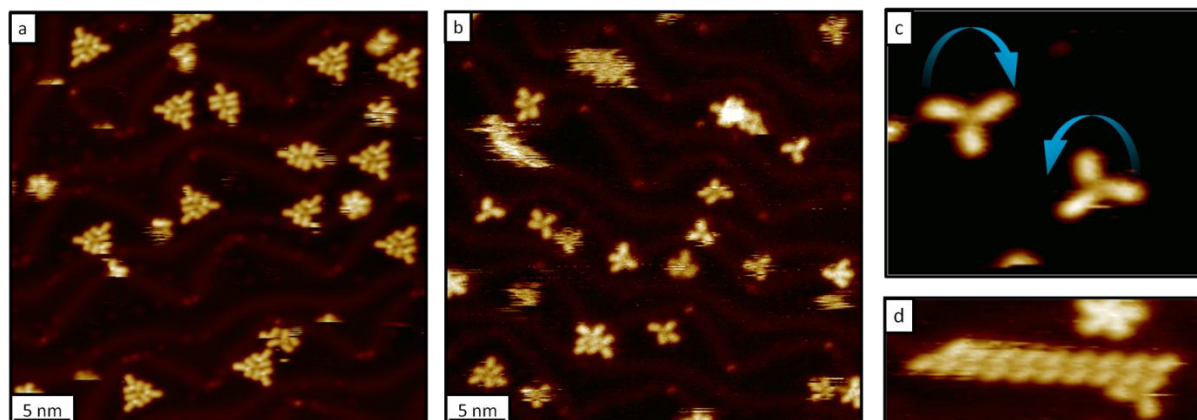

Figure ESI.10. (a) NEP and (b) biphenylcarboxylic acid deposited onto Au(111) at room temperature. The core of the triangular structures in (a) are the same as the three pronged stars from (b). (c) *R*- and *S*-organisational chiralities of the three pronged stars. (d) 2D chain structure of biphenylcarboxylic acid on Au(111). The images were acquired at -196°C.

ESI References

[ESI.1]   Matharu, D. S.; Morris, D.J.; Kawamoto, A. M.; Clarkson, G. J.; Wills. M. *Org. Lett.* **2005,** *7,* 5489-5491.

[ESI.2]   Xu, Y.; Alcock, N. W.; Clarkson, G. J.; Docherty, G.; Woodward, G.; Wills, M. *Org. Lett*. **2004**, *6*, 4105.

[ESI.3]   M. Hayes, D. J. Morris, G. J. Clarkson, M. Wills, *J. Am. Chem. Soc*. **2005**, *127*, 7318–7319.

[ESI.4]   J. W. Evans, M. S. Wainwright, N. W. Cant and D. L. Trimm, *J. Catal.*, 1984, **88**, 203-213.

[ESI.5]   M. A. N. Santiago, M. A. Sánchez-Castillo, R. D. Cortright and J. A. Dumesic, *J. Catal.*, 2000, **193**, 16-28.

[ESI.6]   I.Horcas, R. Fernandez, J. M. Gomez-Rodriguez, J. Colchero, J. Gomez-Herrero *and A. M.* Baro, *Rev. Sci. Instrum.*, 2007, **78**.

[ESI.7]   D. S. Martin, R. J. Cole and S. Haq, *Phys. Rev. B*, 2002, **66**, 155427.

[ESI.8]   T. Classen, M. Lingenfelder, Y. Wang, R. Chopra, C. Virojanadara, U. Starke, G. Costantini, G. Fratesi, S. Fabris, S. de Gironcoli, S. Baroni, S. Haq, R. Raval and K. Kern, *.J. Phys. Chem. A*, 2007, **111**, 12589-12603.

[ESI.9]   D. B. Dougherty, P. Maksymovych and J. T. Yates, Jr., *Surf. Sci.*, 2006, **600**, 4484-4491.

[ESI.10] Y. Wang, S. Fabris, T. W. White, F. Pagliuca, P. Moras, M. Papagno, D. Topwal, P. Sheverdyaeva, C. Carbone, M. Lingenfelder, T. Classen, K. Kern and G. Costantini, *Chem. Commun.*, 2012, **48**, 534-536.

[ESI.11] B. G. Frederick, M. R. Ashton, N. V. Richardson and T. S. Jones, *Surf. Sci.*, 1993, **292**, 33-46.

[ESI.12] L. Grill, M. Dyer, L. Lafferentz, M. Persson, M. V. Peters and S. Hecht, *Nat. Nanotechnol.*, 2007, **2**, 687-691.

[ESI.13] M. W. Schmidt, K. K. Baldridge, J. A. Boatz, S. T. Elbert, M. S. Gordon, J. H. Jensen, S. Koseki, N. Matsunaga, K. A. Nguyen, S. J. Su, T. L. Windus, M. Dupuis and J. A. Montgomery, *J. Comput. Chem.*, 1993, **14**, 1347-1363.